ELECTROTHERMAL LAUNCHERS

An electrothermal (ET) launcher uses electrically heated gas to accelerate projectiles to high velocities. The gas is heated to very high temperatures and pressures in a short time to provide the accelerating force at, or near, the base of the moving projectile. The launcher has a breech region which contains the electrical heating mechanism, and a barrel which contains the projectile and into which the high pressure gas expands. Thus the ET launcher can be thought of as a gun which uses electrical energy instead of chemical propellant to create the high gas pressure to accelerate the projectile. The primary advantage of the ET launcher is a higher projectile velocity for a given energy input. This is accomplished by controlling the timed profile of electrical power to make the launch sequence more efficient. A disadvantage of ET launchers is the large amount of electrical energy storage and switching required for a large gun system. In more advanced designs electrothermal sources and chemical propellants are combined to yield efficient launchers that use a minimum amount of electrical energy.

Light atomic weight gases (hydrogen, helium, etc.) are attractive as a projectile propellant because of a low specific heat and higher sound speed for a given gas temperature. Mechanical pistons have been used to generate the high pressures for acceleration in light-gas guns. Ohmic heating of the gas to high temperatures with or without the pistons has been used to enhance the accelerating pressure since the 1950s. In the late 1970s it was found that higher pressure gases could be formed directly with a relatively simple ohmically heated device called an ablation-controlled arc (1,2). This device has become the basis for ET launcher work to this day. The advantage of an ablation-controlled arc is that no external gas feed is required to form the high temperature gas as will be explained later. Temperatures of the arc are high enough to not only dissociate molecules into individual atoms but to excite and ionize the gas atoms themselves to form a high pressure plasma. The plasma turns out to be in a state of thermodynamic equilibrium (among plasma species) and ohmically heated by an electrical circuit and hence the name *electrothermal* plasma. Unfortunately, ablating plasmas contain significant quantities of higher atomic weight species such as carbon and oxygen.

ELECTROTHERMAL PLASMAS

An electrothermal plasma is a form of an ionized gas similar to that in the sun and stars, except it is characterized by its high density and low plasma temperature. An ET plasma is generated in a confined volume, for example, a capillary, by an ablation mechanism that utilizes electrical energy dissipation from an internal arc. Arc-driven plasmas can be generated over a wide range of pressures, from vacuum conditions to atmospheric to high pressure discharges. An arc plasma is characterized by its high current density. Because plasmas conduct electric currents, the energy dissipation is similar to that of a simple resistor when a current is passing through the resistor known as ohmic or joule dissipation. Such arc-driven plasma may be used to launch projectiles because of the high pressure gradient developed inside the confined volume. The ET plasma is characterized by its temperature, pressure, flow velocity, density, and other important plasma parameters. An ET plasma has a high-density (10^{24} to $10^{27}/m^3$) and temperatures of 1 eV to 5 eV (1.0 electron volt, eV, is equivalent to 11,600 K) (1–4). Figure 1 shows a schematic drawing of an arc-driven electrothermal plasma source that works on the theory of ablation-controlled arcs, where an electric arc is initiated between the cathode and the anode when the switch is closed. The arc extends inside the confined volume, which has an ablating wall ablator such that the ablated material (usually a plastic) is vaporized then ionized because of the heat generated from the arc. The plasma travels inside of the source and is allowed to expand at the source exit. Such arc-driven plasma source is known as "ablation-controlled arc (ACA) source," with typical dimensions of 4 mm to 50 mm bore diameter and 8 cm to 15 cm channel length. When attaching an expansion tube to the source that acts as a launcher barrel, the plasma continues to travel through the barrel and accelerates the mass payload until it leaves the barrel.

ELECTROTHERMAL DEVICES

Figure 2 shows a simplified schematic of an ET launcher, where the plasma source is attached to an expansion barrel that contains the mass to be accelerated. Examples of the kind of projectiles accelerated range from very small to very

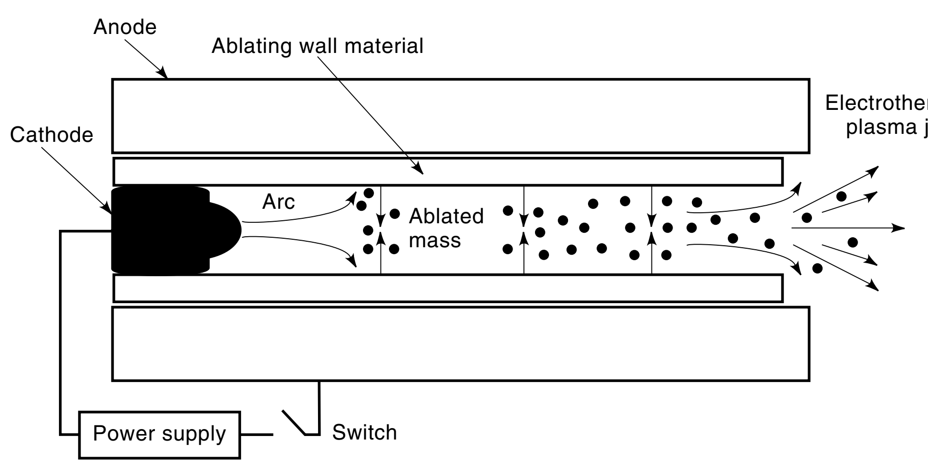

Figure 1. Schematic drawing of an arc-driven electrothermal plasma source based on the theory of ablation-controlled arcs. The arc ablates the liner material, which immediately dissociates, then ionizes and forms the plasma.

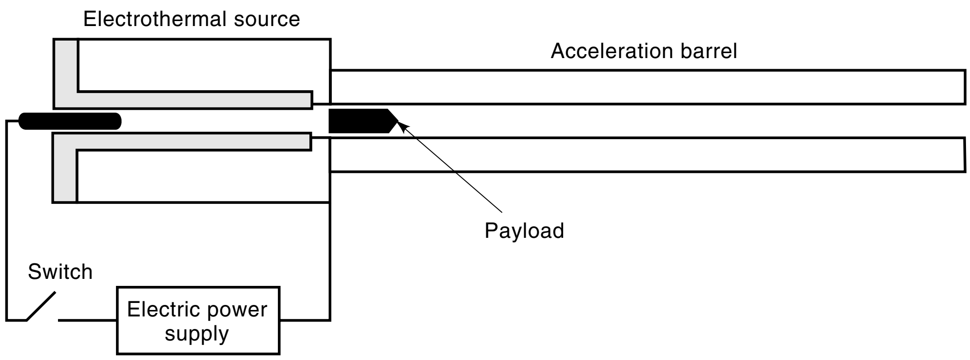

Figure 2. Simplified schematic of an electrothermal launcher showing an electrothermal plasma source attached to an expansion barrel that contains the mass to be accelerated.

large. Frozen hydrogen pellets of only a few milligrams can be launched with an ET injector to fuel a fusion reactor (3). Electrothermal plasma injected into the breech of an electromagnetic launcher railgun, forms an armature to accelerate projectiles of tens of grams.

In another launcher concept, an electrothermal plasma is injected into a chamber that contains a propellant, solid or liquid, where the plasma ignites and controls the burn of the propellant (4,5). Electrochemical-chemical (ETC) launch concepts provide several advantages among other electrothermal plasma launchers, especially for large payloads of several kilograms. It provides a considerably lower gas temperature in the barrel, and thus reduces bore erosion and thermal loading. Additionally, it requires less electrical energy from the external pulse power system because the energy is only used to produce the plasma in the electrothermal injector, which then ignites and controls the burn rates of the chemical propellant. Such an electrothermal-chemical launch concept is already providing the near-term, large scale application of electrothermal launch technology. Figure 3 shows a schematic of the electrothermal-chemical launcher concept, where the basic components are an electrothermal plasma injector, a combustion chamber that contains the propellant, and the barrel that contains the projectile (payload).

POWER SUPPLIES

The electrothermal plasma injector is powered via an external electric power supply, as previously shown in Fig. 1. This pulse power system has a pulse forming network (PFN; see PULSE SHAPING CIRCUITS) composed of energy storage capacitors and coupling inductors. A simple pulse power system, with pulse forming network is shown in Fig. 4, where capacitor modules are coupled to each other via inductors to form the desired pulse length of the discharge current. As shown in the figure, a coupling inductor L is connected between each two capacitors C, and a charging resistor R is connected to the charging high voltage power supply. Coupling to the load (the plasma source) is provided via a high-voltage high-cur-

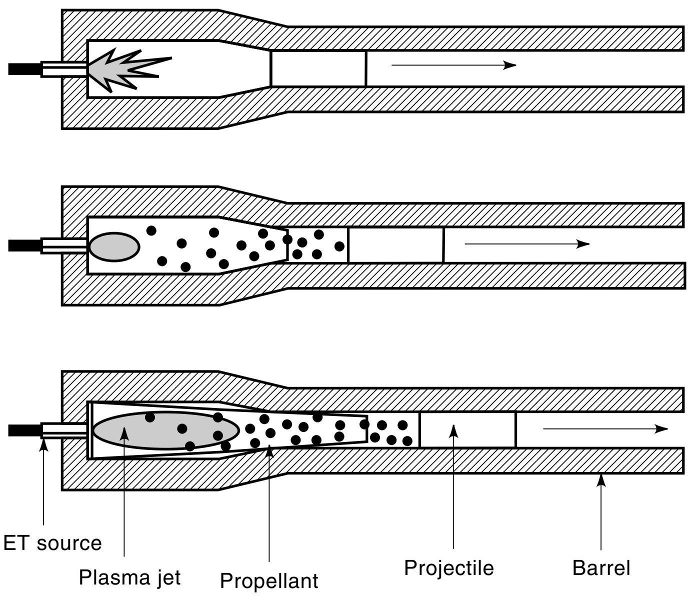

Figure 3. Schematic of the electrothermal-chemical launcher concept showing basic process of plasma injection, propellant's burn and combustion, and motion of the projectile down the barrel. Basic components are an electrothermal plasma injector, a combustion chamber that contains a propellant, and a barrel that contains a projectile.

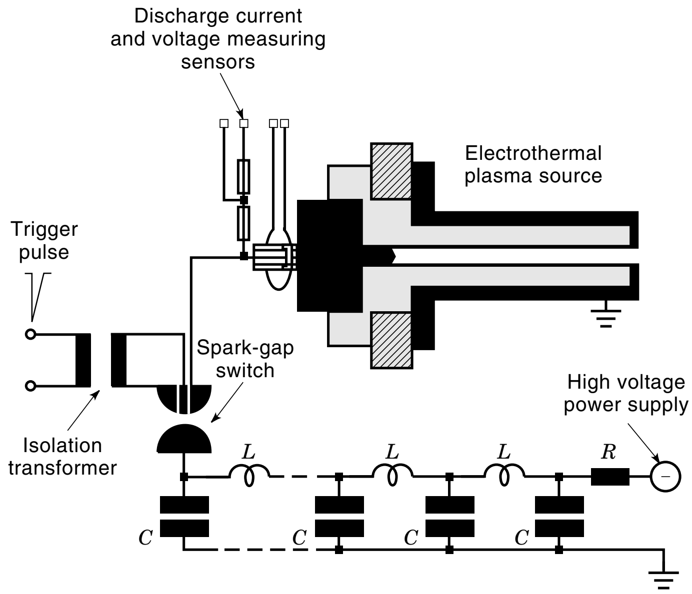

Figure 4. A simple pulse power system with pulse forming network (PFN). Capacitor modules are coupled to each other via inductors to form the desired pulse length of the discharge current. Coupling inductors are connected between the capacitors, and a charging resistor is connected to the charging high voltage power supply.

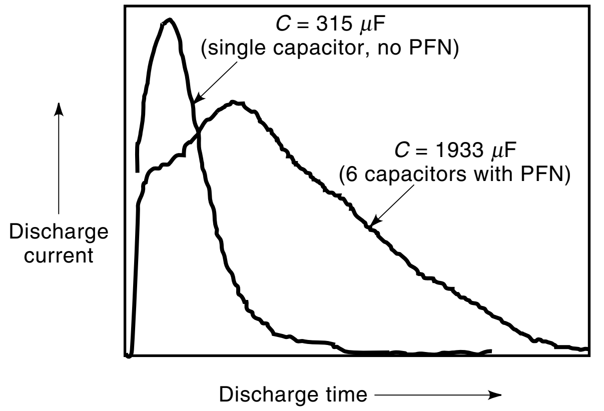

Figure 5. Illustration of how a pulse forming network shapes the discharge current. Two typical time histories of the discharge current are shown, one for a single capacitor of 315 μF without PFN, and one for a PFN composed of six capacitors of 1933 μF total capacitance. Scales are arbitrary.

rent switching device. Because the pulse power systems are designed to deliver high discharge currents, at high charging voltages, special switching is necessary to close the circuit between the energy storage system and the load (the electrothermal plasma injector). Switching may be provided via a simple spark-gap switch that is triggered by a high voltage pulse, or other electronic switching devices such as ignitrons. A high voltage trigger pulse initiates the spark-gap switch, and an isolation pulse transformer is used to isolate the trigger generator from the electric circuit of the spark-gap and the source. Also shown in the figure are two essential measuring tools, a potential divider to measure the discharge voltage across the source V_d, and a current transformer known as a Rogowskii coil to measure the discharge current flowing into the source I_d. Currents of several thousands of amperes could be generated with pulse lengths from as short as a few microseconds (μs) to as long as several milliseconds (ms). Figure 5 illustrates how a pulse forming network shapes the discharge current. Shown in the figure are two typical time histories of the discharge current, one for a single capacitor of 315 μF without PFN where the pulse length is short and has a narrow peak, and one for a PFN (typical to that of Fig. 4) composed of six capacitors of 1933 μF total capacitance where the pulse length is longer and has a wider peak.

It is best to obtain current pulses with a flat top over a longer period of time to provide a similar plasma pressure time history into the source. The reason for flat-top pressures is to achieve near-ideal electrothermal interior ballistics profiles. Ideal electrothermal interior ballistics profiles would have a flat-top plasma pressure, an increasing velocity during the discharge cycle across the source, a slowly increasing temperature (but kept as low as possible), and an increased electric power delivery to the source. The idealistic profiles are shown in Fig. 6, where the pressure is maintained constant over the discharge cycle, and the electric power is increasing until the end of the flat-top pressure then decreases rapidly at the end of the discharge. Neither the pressure nor the temperature will be ideal because the plasma temperature is a function of plasma resistivity, which is governed by collisional processes (electron–ion and electron-neutral collisions), as will be shown in a following section. The temperature, in reality, will increase and decrease following closely the time history of the discharge current. However, maintaining a near flat-top discharge current would also maintain a near constant plasma temperature.

Plasma initiation in electrothermal sources may be achieved via exploding a fuse inside of the capillary (required at initial atmospheric conditions). This is a desired operational regime since an electrothermal launcher is not expected to operate under vacuum. In vacuum, with a back-filling gas, arc initiation is achievable depending on the breakdown conditions as is the case in most glow discharges and vacuum arcs. When operation at atmospheric pressure is desired, the breakdown voltage would be extremely high; thus an exploding fuse would be necessary to achieve breakdown at considerably low voltages. Once the fuse is exploded, it vaporizes and forms a vapor plasma that is immediately ionized. Energy dissipation in the form of ohmic heating continues during the current discharge cycle, and the plasma deposits energy on the inner wall of the ablating surface; thus continuous ablation takes place.

Current large caliber test fixture ETC devices utilize fuse operation of the plasma source. The source may also be designed in various configurations. For example thermo-energy cartridges may be used as plasma igniters for the propellants. The plasma source for ETC launchers may be a simple cartridge attached to the combustion chamber to inject the plasma into the chemical propellant as previously shown in Fig. 3, or be designed in such a way that allows the plasma to flow through the propellant via distributed thin channels (known as piccolo configuration). A piccolo configuration would allow for a better plasma mixing with the propellant, better energy deposition into the propellant, and a better uniform burn (4). The main features of electrothermal plasmas in ETC launchers are to provide augmentation and controllability of burn rates of the propellant. Propellants are typically nitrogen-based compounds not unlike current large gun propellants. Conventional 127 mm (5 in.) bore guns have been

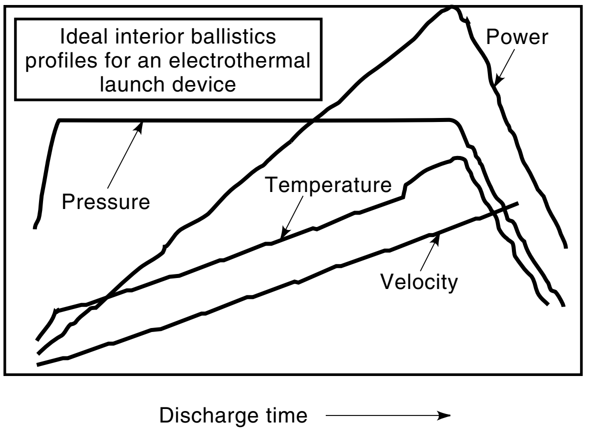

Figure 6. Ideal interior ballistics profiles for electrothermal launch devices. Ideally, the pressure should be maintained constant during the discharge cycle, discharge voltage should be near-linearly increasing, temperature slowly increasing, and the power increasing then decreasing at the end of the cycle. Scales are arbitrary.

modified to use ETC charges. Electrothermal energies approaching a megajoule have been shown to significantly increase the muzzle velocities of projectiles as compared to pure chemical propellants.

ELECTROTHERMAL PLASMA MODELING

Electrothermal plasmas have various applications in launch technology. An electrothermal plasma source may be used as a launcher by itself, or as a pre-injector to form a plasma armature in railguns. In plasma-chemical launchers, the source injects the plasma into a propellant to ignite and control the burn rate and combustion of the propellant. At such plasma temperatures and densities, where plasma radiates energy like a blackbody, an electrothermal plasma can also be used as a high heat flux source for materials evaluation when surfaces are exposed to thermal shocks, as described by Bourham and Gilligan (6,7). A system of equations describing the physics of electrothermal plasmas is illustrative. These equations may be written in a global fashion to calculate the time and spatial-averaged plasma parameters. A global, time-dependent set of equations would help in evaluating the time variation of the plasma parameters, as shown by many researchers (see 8–10). However, a one-dimensional, time dependent description yields a more accurate description that shows the time and spatial variation of the plasma parameters inside the plasma generator, and the plasma flow and acceleration mechanism of the payload inside the launcher's barrel (11,12). The basic equations are the conservation of mass, momentum, and energy. In a simple description, the set of equations describes the balance of masses, momentum and energy from the initiation of the plasma inside of the plasma source and through its travel into the barrel until leaving the muzzle. These balances must also include the projectile motion and acceleration through the barrel. The one-dimensional, time-dependent description is more appropriate because of the nature of plasma initiation in the injector and then its travel along the axial direction into the barrel. A description of the set of equations for an electrothermal plasma injector that is operating on the principles of ablation-controlled arcs is given below for a simple capillary discharge attached to a barrel that contains a payload. When the arc is initiated inside of the capillary, as previously described in Fig. 1, the arc heats the walls of the capillary, ablates materials from the wall, and forms the plasma. One can divide the source and barrel sections into a specific number of cells and look to the plasma as a viscous fluid. Some simplifying assumptions are considered. Each cell is considered to be at local thermodynamic equilibrium because the plasma has a high density and considerably low temperature, and thus it is highly collisional. The fluid equations are nonlinear due to the ionization, radiation, and drag effects. The specific internal energy of the plasma is a function of the temperature assuming that the ablated material is completely dissociated. A mechanism known as the vapor shield will also be considered. This mechanism provides a self-protecting nature to the ablating wall because the evolved vapor cloud absorbs a fraction of the arc energy such that the net energy reaching the wall will be reduced (13). This mechanism will be described in more detail in the plasma-materials interaction section. Because of the one dimensionality, the plasma parameters are assumed to be constant across the cross section of the capillary and the barrel. The ablated material in the source is assumed to be totally dissociated into the constituent atoms. The heat loss due to conduction inside both the source and the barrel is assumed to be negligible. Also, the axial radiation transport is assumed to be negligible inside the source where the plasma temperature is fairly isothermal. Additional assumptions will be introduced, whenever necessary, throughout the description of the set of equations.

Conservation of Mass

The rate of change in the particle density in each cell is the difference between the rate at which particles are introduced into the cell from ablation of the wall and the rate at which particles enter and leave the cell. The equation of continuity for each cell is given in (14) by:

$$\frac{\partial n}{\partial t} = \dot{n}_{\mathrm{a}} - \frac{\partial (vn)}{\partial z} \tag{1}$$

where n is the number density of plasma particles (atoms/m^3), v is the plasma velocity (m/s), and is the time rate of change of the number density of ablated material from the cell wall (atoms/m^3 s) and is given in (15) by:

$$\dot{n}_{\mathrm{a}} = \frac{2q''}{H_{\mathrm{sub}} A_{\mathrm{p}} R} \tag{2}$$

where q'' is the radiation heat flux incident on the wall surface (W/m^2), A_{p} is the mass of the atoms that constitute the plasma (kg/atom), R is the radius of the cell (meters), and H_{sub} is the sum of the energy of dissociation of the molecules to the constituent atoms (the heat of sublimation and vaporization). The radiation heat flux incident on the wall surface is a fraction of the blackbody radiation emitted from the hot plasma core, and is given by:

$$q'' = f \sigma_{\mathrm{s}} T^4 \tag{3}$$

where f is the energy transmission factor through the vapor shield, σ_{s} is the Stefan–Boltzmann constant (5.670×10^{-8} W/m^2 K^4), and T is the plasma temperature (K). The energy transmission factor, f, is a function of the heat of sublimation H_{sub}, plasma internal energy, plasma pressure and density (14,15).

Conservation of Momentum

The change in velocity in each cell is due to the pressure forces, the kinetic energy of particles entering and leaving the cell, and the ablation and viscous drags. The equation for the time rate of change of the velocity in each cell is given in (14,15) by:

$$\frac{\partial v}{\partial t} = -\frac{1}{\rho}\frac{\partial P}{\partial z} - \frac{1}{2}\frac{\partial v^2}{\partial z} - \frac{v\dot{n}_{\mathrm{a}}}{n} - \frac{2\tau_{\mathrm{w}}}{\rho R} \tag{4}$$

where τ_{w} is the viscous drag at the wall (N/m^2). In a simplistic steady-state way, the momentum equation can be expressed by the first term on the right-hand side equal only to the first term on the left hand side, means that the rate of change of velocity is equal to the change in velocity due to the axial pressure gradient, with opposite sign. But due to axial dependence, the momentum equation must include additional terms as appearing on the right hand side of Eq. (4). The second term is the change in velocity due to the kinetic energy gradient. The third term is the velocity loss due to the increase in the number density from ablated material (ablation drag).

When setting the momentum equation for the barrel, one has to include an additional term on the right hand side of Eq. (4) to account for losses due to momentum transfer to the payload (projectile). This additional term has to be added negatively to the right-hand side of the equation and is given in (12) by:

$$\frac{\rho_{\text{proj}}}{\rho}\frac{\partial v_{\text{proj}}}{\partial t} \tag{5}$$

Conservation of Energy

The rate of change of the internal energy in each cell in the plasma source section is due to joule heating, radiation, flow work, changes in density, internal energy entering or leaving the cell due to particle transport, and frictional heating. The time rate of change of internal energy in each cell in the source is given in (14,15) by:

$$n\frac{\partial U}{\partial t} = \eta j^2 - \frac{2q''}{R} - P\frac{\partial v}{\partial z} + \frac{1}{2}\dot{\rho}_a v^2 - \dot{n}_a U - v\frac{\partial (nU)}{\partial z} \tag{6}$$

where η is the plasma resistivity (Ω-m), and j is the discharge current density (A/m^2). The first term on the right-hand side is the increase in internal energy due to joule heating. The second term is the loss in internal energy due to thermal radiation and the $(2/R)$ factor is due to the conversion of surface heat flux to volume radiation. The third term is the change in internal energy due to work done by the plasma (flow work). The fourth term is the increase in internal energy due to friction from ablation. The fifth term is the loss in internal energy due to the cold ablated material entering the plasma. The sixth term is the change in internal energy due to particles entering and leaving the cell. When setting the energy equation for the barrel, one has to remove the joule heating term, and include a term to the right hand side of Eq. (6) to account for loss of internal energy which is transferred to the energy of the payload (projectile). This additional term has to be added negatively to the right hand side of Eq. (6) and is given in (12) by:

$$\rho_{\text{proj}} v_{\text{proj}} \frac{\partial v_{\text{proj}}}{\partial t} \tag{7}$$

The energy equation includes several terms that need to be defined. The internal energy, for an ideal plasma, is given in (15) by:

$$U = 1.5kT(1+\overline{Z}) + \overline{I} + H_{\text{sub}} \tag{8}$$

where the first term on the right-hand side is the internal energy due to thermal motion, and the second term is the internal energy due to ionization. The modified Saha–Boltzmann equation gives the relation between the effective charge state and the ionization potential, and is given in detail in (16). The plasma resistivity, which appears in the joule heating term must be a summation of two resistivities due to electron-neutral and electron-ion collisions $\eta = \eta_{en} + \eta_{ei}$, where the resistivity due to electron-neutral collisions is given in detail by Cambel in (17). The resistivity due to electron-ion collisions could be determined using the Spitzer resistivity model, as given by Spitzer and Harm in (18).

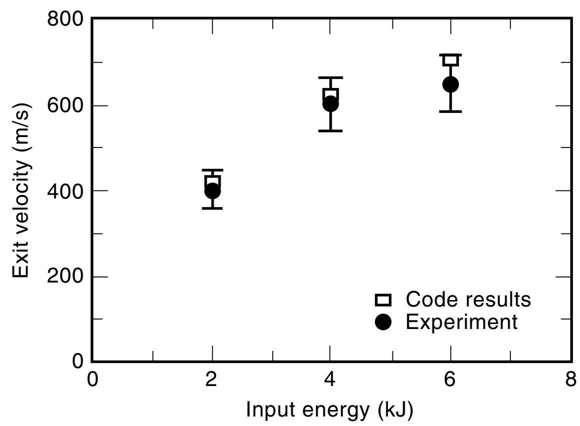

Figure 7. A comparison between experimental and computer code results for the exit velocity of a half gram projectile accelerated in a 15 cm barrel using an electrothermal launcher.

Modifications to the Spitzer resistivity for high-density, low-temperature plasmas are better introduced because such electrothermal plasmas tend to be weakly nonideal such that the ideal resistivity model will no longer be valid, as shown by various researchers in (19,20). Also, the plasma viscosity has to be the summation of two viscosity terms, the viscosity due to the neutral atoms, and that due to the ions. It is apparent that the given set of equations has to be solved self-consistently. Although a time-averaged and spatially-averaged analytical solution may be obtained with additional simplifying assumptions, a complete self-consistent one-dimensional time-dependent solution has to be obtained numerically via appropriate computer codes. Many computer codes have been developed for electrothermal plasmas in launch devices to solve the set of governing equations self consistently and to help predict the plasma parameters for a given discharge configuration and current profile. An example of the computer code results for the exit velocity of a half gram projectile accelerated in a 15 cm barrel is shown in Fig. 7 together with experimental measurements. The velocity reaches 700 m/s for an input energy of 6 kJ to the electrothermal plasma source.

PLASMA-MATERIAL INTERACTION

In most electric launch devices (electrothermal, electrothermal-chemical, and electromagnetic), the heat flux from the arc-formed plasma may exceed 100 GW/m^2 for a duration of 0.01 ms to 5 ms. As a result, critical components are damaged due to surface erosion and thermal deformations. Surface erosion is one of the parameters that has an effect on the performance, durability, efficiency, and lifetime of the launch device. Minimum deformation and damage of the critical com-

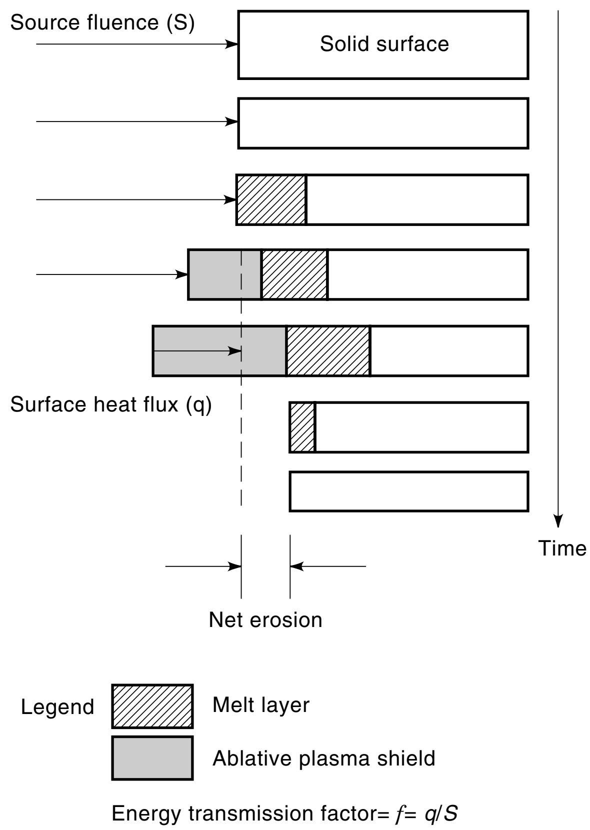

Figure 8. A time history illustration of the vapor shield mechanism. The plasma energy is deposited on the surface and raises the temperature. The surface melts then vaporizes. The incoming energy is deposited in the developed vapor layer and less energy reaches the surface. The heat flux that reaches the surface is a fraction of the source fluence. At the end of the cycle, the melt layer re-solidifies leaving a final net surface erosion. Time scale is arbitrary.

ponents are required in order to achieve efficient operation of the launcher, especially at high repetition rates of operation. High thermal resistance materials may help in reducing surface erosion of the launcher components. A possible approach is to use refractory materials or refractory coatings on materials to reduce surface erosion of rails and barrels; also high tensile insulating materials and specially prepared composites may also be considered to eliminate the ablation of the insulators in railguns and electrothermal plasma injection sources (21–25).

Under such short and intense high heat flux conditions the material surface suffers melting and vaporization, and a plasma boundary layer will be formed at the ablating surface. Such vapor plasma absorbs a fraction of the incoming energy; thus less heat flux reaches the surface resulting in less surface erosion. This is described as the vapor shield mechanism, and is schematically illustrated in Fig. 8. The energy absorbed in the vapor layer appears as internal energy that can be transported away from the localized area due to the large pressure (>1 kbar; 1 kbar is 1000 times atmospheric pressure), which is large enough to expand against an incoming plasma flux (26). The heat flux is primarily from blackbody spectrum photons, as previously given by Eq. (3). Once the energy is deposited in the vapor layer then low energy photon transport becomes the dominant mechanism by which energy is transferred to the material surface (21,25). The plasma flow in such devices has a Reynolds number of 10^5 to 10^7, and consequently the viscous skin friction generates turbulence.

Experiments on various materials have been conducted using varieties of launch devices and simulators to explore the performance and response of such materials to high heat fluxes produced from arc-driven plasmas. For example, pure copper and gunsteel have approximately equal erosion, which is about 60% less than that of aluminum. Molybdenum is even better and has about 75% less erosion than aluminum, while tungsten has no obvious erosion below 20 GW/m^2, but surface coloration and micro cracks may occur. Because refractory materials have less surface erosion, better thermal resistance, and better structural strength, launcher components may be coated with layers of selected refractory materials. Graphite and carbon materials have no melting temperature when direct sublimation takes place.

The energy transmission factor through the vapor shield is the ratio between the actual heat flux at the ablating surface to the incident heat flux from the plasma source, which is about 10% for most graphite grades at incident heat fluxes of 60 GW/m^2 and greater. Insulators are important materials for electrothermal and all electrically driven launch devices. Many polymer materials have been considered as insulating components in electrothermal launch devices, among these is Lexan, which is a polycarbonate polymer ($C_{16}H_{14}O_3$). The vapor shield is more effective for highly ablating materials due to the fast development of the vapor layer. Lexan, boron nitride, and aluminum oxide have approximately equal energy transmission factors, while silicon carbide composite is approximately a factor of two higher (25). A comparison between the energy transmission factor for three insulators, Lexan polycarbonate, boron nitride, and silicon carbide, is illustrated in Fig. 9 showing a decreased factor for increased heat

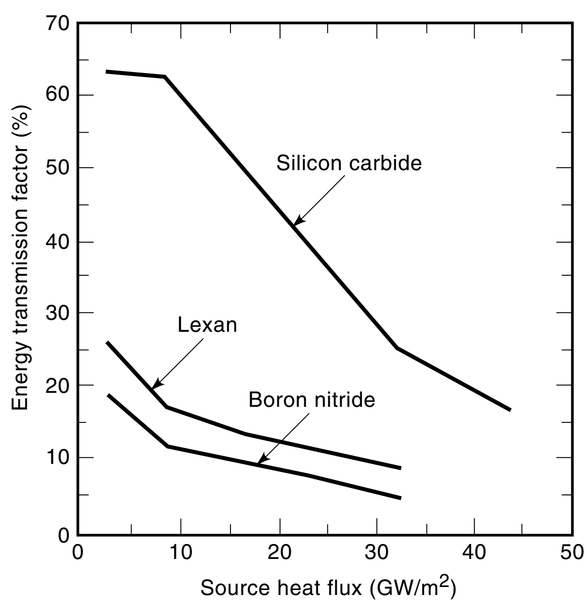

Figure 9. A comparison between the energy transmission factor for three insulators, Lexan polycarbonate, boron nitride, and silicon carbide, showing a decreased factor for increased heat flux.

Table 1. Erosion Thickness of Various Materials Exposed to High Energy Electrothermal Plasmas

Input Energy to Electrothermal Plasma Source (kJ) =>	1	2	3	4	5	6	7
Heat Flux from Electrothermal Plasma Source (GW/m^2) =>	2.8	8.6	15.6	23.6	32.5	43.8	59.4
Material	Erosion Thickness (μm)						
Aluminum	10.6	47.3	99.8	168	206		
Titanium	7.1	49.6	89.8	114	153	215	260
Gun steel					57.7		
Copper	2.6	12.7	24.1	36.4	52.8		
Molybdenum (arc cast)	0.1	0.9	9.7	19.2	32.8		
Molybdenum (sintered)	0.2	3.5	28.2	15.6	30.9		
Glidcop (Cu- 0.15% Al_2O_3)	1.8	9.8	19.9	22.5	28.3		
Molybdenum on copper					18.8		
Tantalum carbide on copper					4.3		
Tantalum nitride on copper					3.8		
Tantalum on copper					0.8		
Tungsten	≈0	≈0	≈0	≈0	≈0		
Tungsten-rhenium alloy (3% Re)	≈0	≈0	≈0	≈0	≈0	≈0	≈0
Lexan (polycarbonate, $C_{16}H_{14}O_3$)	11.1	23.3	30.8	41	43.5		
Boron nitride (grade A)	5.2	10.5	15.7	20.6	20.1		
Glass-bonded mica	1.2	6.0	8.5				
Annealed pyrographite (P-ANN-PG)					12.8		
Molded dense electrographite (2020)	≈0	1.1	1.9	11.4	6.8		
High density graphite (6222)	≈0	≈0	≈0	3.7	3.3	5.2	9.4
Highly anisotropic pyrographite	2.7	3.6		2.4			

flux. This factor is about 10% for most materials at higher heat fluxes. A summary of measured erosion thickness of various materials exposed to high energy electrothermal plasma is given in Table 1, for heat fluxes up to 60 GW/m^2 over a 100 μs pulse length.

BIBLIOGRAPHY

1. E. Z. Ibrahim, The ablation dominated polymethylmethacrylate arc, *J. Phys. D.: Appl. Phys.,* **13**: 2045–2065, 1980.
2. C. B. Ruchti and L. Niemeyer, Ablation controlled arcs, *IEEE Trans. Plasma Sci.,* **14**: 423–434, 1986.
3. R. W. Kincaid, M. A. Bourham, and J. G. Gilligan, Electrothermal plasma gun as a pellet injector, *Fusion Technol.,* **26**: 637–641, 1994.
4. W. F. Oberle, Technology efforts in ETC gun propulsion. Army Research Laboratory, ARL-SR-12, 6, 1-309, 1994; ARL-SR-22, 7, 1-191, 1995; *Proc. JANNAF Combustion Meetings:* CPIA 573, I, 165, 1991; CPIA 593, I, 299, 1992; CPIA 606, I, 17-25, 1993; CPIA 602, I, 17-21, 1994.
5. D. Hewkin and E. Figura, Fundamental research and numerical modeling of the internal ballistics of electrothermal chemical guns, *IEEE Trans. Magn.,* **29**: 561–566, 1993.
6. M. Bourham et al., Electrothermal plasma source as a high heat flux simulator for plasma-facing components and launch technology studies, *Proc. 9th International Conference on High Power Particle Beams,* Washington, DC, May, 1992, **III**: 1979–1983, 1992.
7. J. Gilligan and M. Bourham, The use of an electrothermal plasma gun to simulate the extremely high heat flux conditions of a tokamak disruption, *J. Fusion Energy,* **12** (3): 311–316, 1993.
8. E. Jacob, S. Bouquet, and B. Tortel, A global theoretical approach for the electrothermal gun: Scaling laws and a 0-D time-dependent model, *IEEE Trans. Magn.,* **31**: 419–424, 1995.
9. S. Cuperman, D. Zoler, and J. Ashkenazy, Analysis of critical flow in a combined discharge capillary-ablative pipe system, *Plasma Sources Sci. Technol.,* **3**: 593–601, 1994.
10. J. D. Powell and A. E. Zielinski, Analysis of the plasma discharge in an electrothermal gun. In A. A. Juhaz (ed.), *Technology Efforts in ET Gun Propulsion,* US Army Ballistic Research Laboratory, Arberdeen Proving Grounds, MD, Vol. II, 1989.
11. J. D. Hurley, M. A. Bourham, and J. G. Gilligan, Numerical simulation and experiment of plasma flow in the electrothermal launcher SIRENS, *IEEE Trans. Magn.,* **31**: 616–621, 1995.
12. R. W. Kincaid, M. A. Bourham, and J. G. Gilligan, Plasma gun pellet acceleration modeling and experiment, *Fusion Technol.,* **30**: 834–839, 1996.
13. M. A. Bourham et al., Vapor shielding and erosion of surfaces exposed to high heat load in an electrothermal accelerator, *IEEE Trans. Plasma Sci.,* **17**: 386–391, 1989.
14. J. D. Powell and A. E. Zielinski, Theory and experiment for an ablating-capillary discharge and application to electrothermal-chemical guns, BRL Tech. Rep. BRL-TR-3355, 1–50, 1992.
15. J. G. Gilligan and R. B. Mohanti, Time dependent numerical simulation of ablation controlled arcs, *IEEE Trans. Plasma Sci.,* **18**: 190–197, 1990.
16. Ya. B. Zeldovich and Yu P. Raizer, *Physics of Shock Waves and High Temperature Hydrodynamic Phenomena,* Vol. 1, New York: Academic Press, 1963.
17. A. B. Cambel, *Plasma Physics and Magneto-Fluidmechanics,* New York: McGraw-Hill, 1963.
18. L. Spitzer, Jr. and R. Harm, Transport phenomena in a completely ionized gas, *Phys. Rev.,* **89**: 977, 1953.
19. R. B. Mohanti and J. G. Gilligan, Electrical conductivity and thermodynamic functions of weakly nonideal plasmas, *J. Appl. Phys.,* **68**: 5044–5051, 1990.
20. J. Batteh et al., A methodology for computing thermodynamic and transport properties of plasma mixtures in ETC injectors, *IEEE Trans. Magn.,* **31**: 388–393, 1995.

21. M. A. Bourham, J. G. Gilligan, and O. E. Hankins, Plasma-material interaction in electrothermal and electromagnetic launchers, *AIAA 24th Plasmadynamics & Lasers Conference,* Orlando, FL, AIAA 93-3172, 1993.
22. F. D. Witherspoon, R. L. Burton, and S. A. Goldstein, Railgun experiments with lexan insulators, *IEEE Trans. Plasma Sci.,* **17**: 353–359, 1989.
23. R. D. Stevenson, S. N. Rosenwasser, and R. M. Washburn, Development of advanced ceramic matrix composite insulators for electromagnetic railguns, *IEEE Trans. Magn.,* **27**: 538, 1991.
24. A. E. Zielinski and C. V. Renaud, Erosion resistance of CuNb microcomposites in a plasma armature electromagnetic launcher, BRL Tech. Rep., BRL-TR-3311, 1–30, 1992.
25. M. A. Bourham et al., Review of components erosion in electric launchers technology, *IEEE Trans. Magn.,* **31**: 678–683, 1995.
26. A. Hassanein, Erosion and redeposition of divertor and wall materials during abnormal events, *Fusion Technol.,* **19**: 1789, 1991.

Reading List

P. Aubouin, Electrothermal launcher plasma burner modeling and comparison to experimental results, *Proc. 4th European Symposium on Electromagnetic Launch Technology,* Germany, 1993, paper 1003.

E. Blums, Yu. A. Mikhailov, and R. Ozols, *Heat and Mass Transfer in MHD Flows,* Singapore: World Scientific Publishing Co., 1987.

J. R. Greig et al., Investigation of plasma-augmented solid propellant interior ballistic process, *IEEE Trans. Magn.,* **29**: 555–560, 1993.

A. Loeb and Z. Kaplan, A theoretical model for the physical processes in the confined high pressure Discharges of electrothermal launchers, *IEEE Trans. Magn.,* **25**: 342–346, 1989.

B. Schmit and Th. H. G. G. Weise, Performance and results of the TZN electrothermal gun simulation code, *Proc. 4th European Symposium on Electromagnetic Launch Technology,* Germany, 1993, paper 1016.

E. Y. Scholnikov et al., High efficiency electrothermal accelerator, *IEEE Trans. Magn.,* **31**: 447–451, 1995.

D. D. Schuresko et al., Development of a hydrogen electrothermal accelerator for plasma fueling, *J. Vac. Sci. Technol.,* **A5** (4): 2194, 1987.

G. P. Wren et al., Spatial effects of an electrically generated plasma on the interior ballistics of electrothermal-chemical (ETC) guns, *IEEE Trans. Magn.,* **31**: 457–462, 1995.

MOHAMED A. BOURHAM
JOHN G. GILLIGAN
North Carolina State University

ELECTROVISCOUS FLUIDS.

See ELECTRORHEOLOGY.